Hobby-Eberly telescope medium-resolution spectrograph

Ramsey, Lawrence

Lawrence W. Ramsey, "Hobby-Eberly telescope medium-resolution spectrograph," Proc. SPIE 2476, Fiber Optics in Astronomical Applications, (14 June 1995); doi: 10.1117/12.211849

SPIE.

Event: SPIE's 1995 Symposium on OE/Aerospace Sensing and Dual Use Photonics, 1995, Orlando, FL, United States

Hobby-Eberly telescope medium resolution spectrograph

Lawrence W. Ramsey

The Pennsylvania State University, Department of Astronomy and Astrophysics.
525 Davey Laboratory, University Park, PA 16802

ABSTRACT

We present a concept design for a versatile, high throughput fiber coupled spectrograph for the 9-meter Hobby-Eberly telescope. This instrument, designated the Medium Resolution Spectrograph (MRS) will cover the visible spectrum from 350 nm to 1100 nm and have a resolution range $3000 < \lambda/\Delta\lambda < 20000$. It will reside in an environmentally controlled spectrograph room. Operating modes of the spectrograph will include single object, synthetic long slit and multiple object spectroscopy. The dual requirements of spectral coverage and high resolution mandate that the MRS be a dual beam instrument.

1. INTRODUCTION

The Hobby-Eberly telescope (HET) marks a fundamental departure from the usual paradigm for building large optical telescopes. Central to the HET approach is specialization: the HET is tailored for spectroscopy, and in particular, fiber-coupled spectroscopy. By limiting observational flexibility, extremely cost-effective technical solutions are possible and these have been implemented in the HET's design which is outlined below. The MRS is a key component of the planned HET instrument suite, which includes a high throughput, low resolution ($300 < R = \lambda/\Delta\lambda < 700$) prime focus spectrograph (LRS), a fiber coupled high resolution ($20000 < R < 60000$) spectrograph (HRS) and imaging capability over the full 4 arc minute prime focus field of view (FoV).

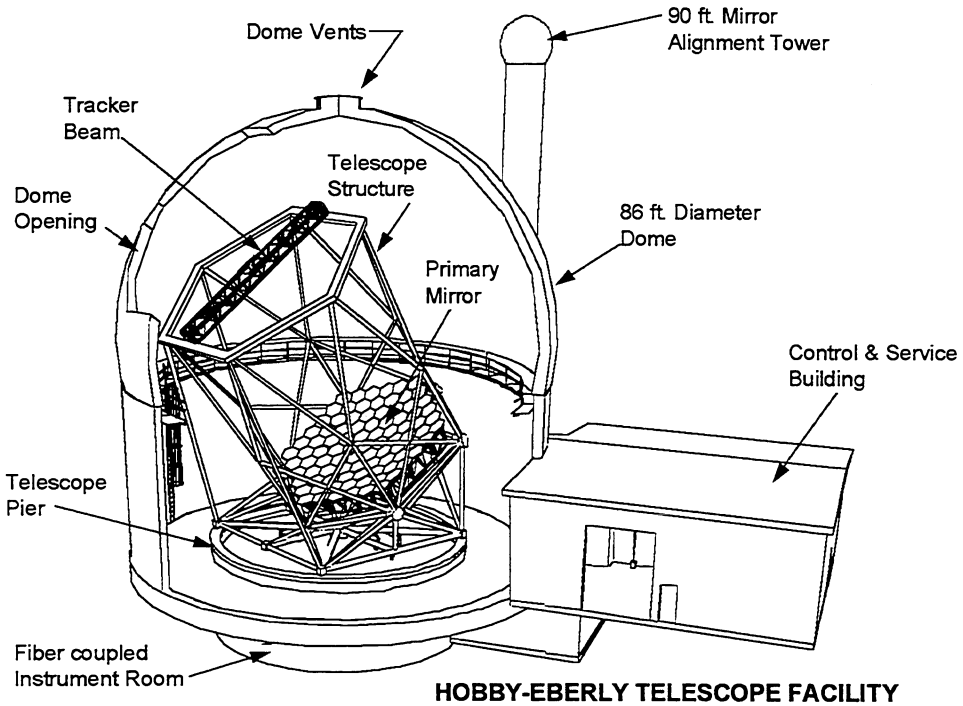

Figure 1: A view of Hobby-Eberly telescope facility. The fixed tilt of the telescope and segmented primary mirror are apparent. The telescope sits on a pier which also serves as an enclosure for a fiber fed spectrograph room. An object is followed in the focal plane of the spherical primary using a six axis tracker system illustrated by the beam on the top of the telescope in this figure.

0-8194-1829-3/95/$6.00

Ramsey et al.[1] and Sebring, et al. [2] have recently described the HET in detail. Figure 1 illustrates the major features of the telescope. The HET has a segmented spherical primary mirror with the central optical axis tilted at a fixed 35° angle. This makes the HET a tilted optical Arecibo type telescope, but with full azimuth freedom, allowing it to access declinations from -10° 20' to +71° 40'(about 70% of what a general purpose telescope at the same site would normally achieve). Thus, rotation in the HET is not a tracking mode, but is critical for pointing and sky access. Motion of an object across the sky is followed by a tracker, which carries the spherical aberration corrector and fiber feed. The tracking time across the 12° focal surface ranges from 0.75 hr. at the equator to 2.5 hr. at the north declination limit[1]. The HET prime focus is a well-corrected and baffled 4 arc minute field behind a Gregorian corrector. The simplicity of this design demands that large instruments, such as the MRS, be fiber coupled.

In the HET, silver coatings are used to deliver ~75% of the light incident on its 9 meter entrance pupil to the focal plane. That includes 16% geometrical obstructions due to primary mirror gaps and bevels, as well as the aberration corrector central obstruction.

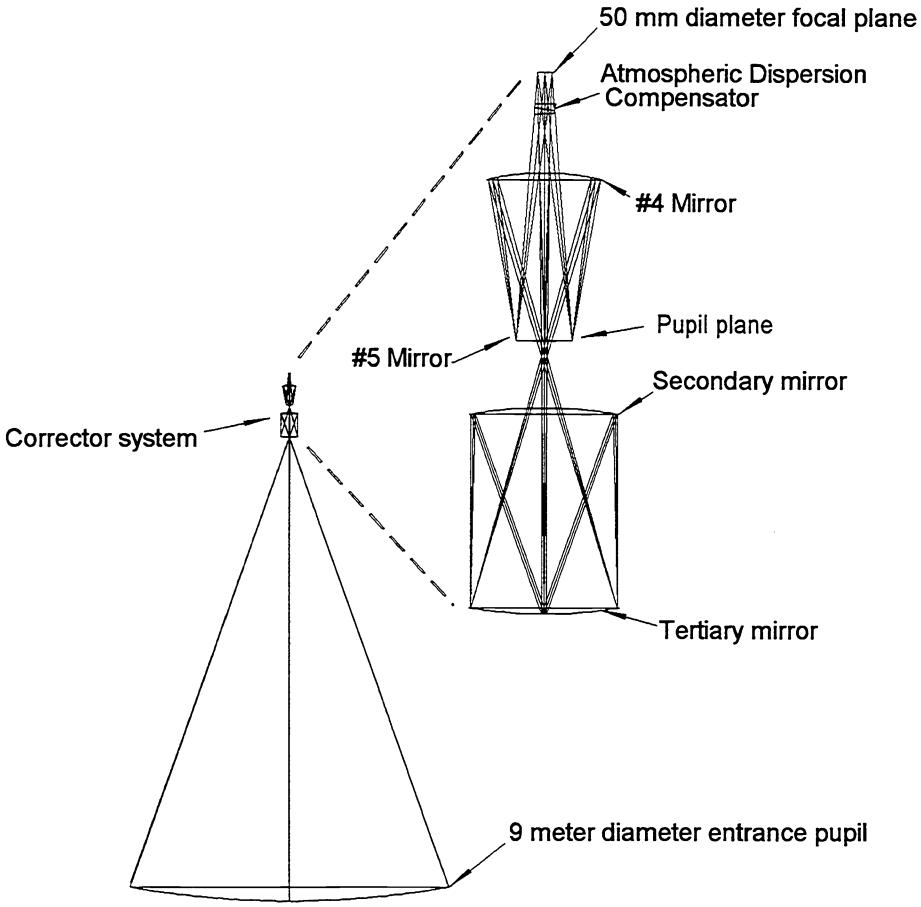

Figure 2: This optical schematic illustrates the essential features of the Hobby-Eberly telescope optical system. The spherical primary mirror has a focal length of 13.08 meters. A all reflecting spherical aberration corrector, shown blown up to the right, delivers the final image to the focal surface with a focal ratio f/4.7 and an image scale of 204.5 microns/arc-sec on the sky.

Figure 2 presents an optical schematic for the HET. The primary mirror is spherical and has a radius of curvature of 26.165 meters. An all reflecting Gregorian corrector removes the formidable amount of spherical aberration present at the prime focus of the primary. The corrector must move across the focal surface, which is as a spherical surface 13.08 meters from the primary mirror center of curvature (CoC), all the time keeping its optical axis aligned with the CoC.

An advantage of a spherical primary mirror is that a point at the CoC is re-imaged at that point. This provides a simple mechanism for alignment of the segments without having to acquire and track a star and to do so in the daytime if desired. The HET facility, discussed in more detail by Sebring et al.[2], includes a tower that allows access to this vital point

An important effect that must be considered in the HET is a changing pupil illumination as an object is tracked across the sky. The corrector defines the pupil size, and it can "see" off the primary mirror when the tracker moves significantly off center. The vignetting resulting when the tracker is significantly off center makes the average aperture of the HET a function of tracking time[1]. For example, the effective aperture remains about 9 meters for short 10 minute tracks near the center of the tracker field, but diminishes to about 7.2 meters in the worst case off axis 40 minute track. This Aspect of the HET demands careful consideration of baffling as well as the scrambling capability of optical fibers.

2. MRS REQUIREMENTS

The MRS will be designed to take maximum advantage of the high efficiency optics and queue scheduled nature of the HET. Among its many science programs, the MRS will 1) explore the broad line regions of active galactic nuclei and quasars through dense time spectroscopy, 2) examine the evolution of large scale structure in the universe through measurements of quasar absorption lines, 3) detect and characterize the properties of dark matter via kinematical measurements in elliptical galaxies, and 4) measure the age and dynamical evolution of the Milky Way through knematical studies of white dwarf stars.

The science programs establish the technical requirements for the MRS. We summarize here the science requirements demanded by the above programs and the far larger list compiled by HET collaborators:

- The MRS must provide fiber-coupled spectroscopic capability in the range $3000 < \lambda/\Delta\lambda < 18000$.
- The MRS must provide full spectral coverage between 350 and 1100 nm.
- The MRS must provide the capability for excellent sky subtraction.
- The MRS must provide dimensional stability consistent with radial velocity precision < 1 km/s.
- Efficiency of >15% on the sky is a priority MRS design goal.
- The MRS must have scattered light less than 2% in the cores of fully saturated absorption lines.
- The MRS must be compatible with high operational efficiency within the HET system; any fiber or spectrograph re-configuration must take 1 minute or less.
- The MRS must have MOS capability, ~10 objects.

3. INSTRUMENTAL APPROACH

The complete MRS system will consist of a fiber feed and a dual beam spectrograph with two detectors. The spectrograph will be a dual, cross dispersed echelle in a white pupil configuration and will utilize large format CCDs at each camera focus. The fiber feed will have three distinct modes: single object, synthetic long slit and multiple object spectroscopy (MOS).

3.1 HET fiber feed approach

The corrected HET prime focus operates at f/4.7. This ratio is a compromise between the effects of focal ratio degradation (FRD) which prefers faster f-ratios[3] and scrambling considerations[4] which favors slower f-values. An atmospheric dispersion corrector (ADC) that has a secondary dispersion of less than 0.2 arc-seconds (") and an efficiency >95% over the 350-1100 nm band-pass is about 120 mm in front of the fiber input. Fibers from this focus, illustrated in Figure 3, will be efficiently routed over a 30 m path from the tracker to a thermally controlled spectrograph room below the telescope. Recent measurements on CeramOptic hydrogenated low OH fibers[5] indicate that a single fiber will meet our requirements. The MRS will be placed on an optical table in this room and operate in a flexure-free environment guaranteeing high dimensional stability and better than 1 km/s radial velocity stability at R=10000.

Brodie et al.[6] and Ingerson[7] discuss strategies for selecting fiber sizes. The key is to consider the ultimate SNR as the figure of merit. In our modeling we used measured seeing profiles[8] and extant CCD properties as opposed to ideal photon counters. Our results are in qualitative agreement with earlier studies but show that the presence of a slight dark or readout noise further broadens the range of optimum apertures when the sky is equal to or greater than the object. We find that three standard core diameters ~1.5", 2", and 3" on the sky will serve all our needs. This is facilitated by using a slit mask at the fiber output to set the operational resolution (see section 3.2). Analysis shows that for all our spectrograph resolution configurations, for either

the photon limited or background limited case, the above selection of fiber sizes differ by no more than 10% in SNR from that obtained with an optimum fiber size.

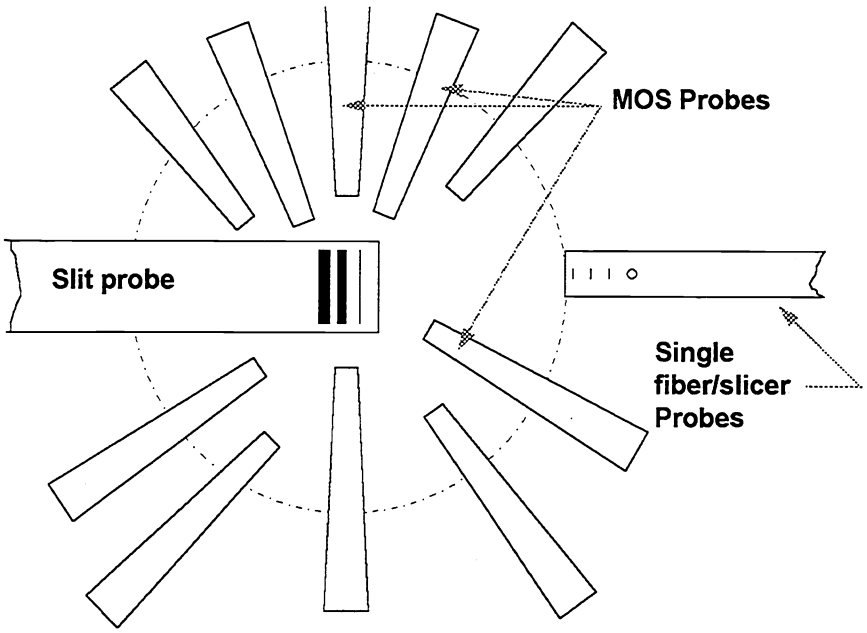

Figure 3: This schematic layout illustrates the essential features of the fiber feed system. The 50 mm diameter 4 arc-minute field of view is outlined by the dotted circle The slit probe and single fiber/slicer probes move in and out whereas the MOS probes move radially and translate so as to each cover about 20% of the field.

3.1.1 Single fiber/slicer probe

This probe will contain three rows of five fibers; one object and 4 sky for each fiber size. An addition position on this probe will be occupied by a 3 arc-second fiber which feeds a special scrambler[9] fiber slicer at the output end at the spectrograph slit. The probe will be carried on a one dimensional stage that will place the desired size fiber at the field center with 10 μm (0.05") accuracy. It is shown in the above figure withdrawn to the edge of the field of view.

3.1.2 Synthetic slit

This probe, detailed in Figure 4, will contain three rows of fibers, 34" on the sky (synthetic long slits), with one row for each fiber size. Field rotation is done by the HET tracker system and allows placement of the fiber array at a selected angle on the sky. The telecentric angle in the focal plane varies by ~1.6° over our field radius and by 0.43° over the 32" array length. This can increase our FRD as a function of fiber position[10]. To keep such losses <3%, each 32" linear array will be composed of 4 blocks; each 8" long and slightly tilted to conform to the local optical axis. The blocks will be optimized to work at the center of the focal plane. This probe will also be positioned on a stage that will place the desired size synthetic slit at the field center with 10 μm (0.05") accuracy and like the single fiber probe, will move only radially.

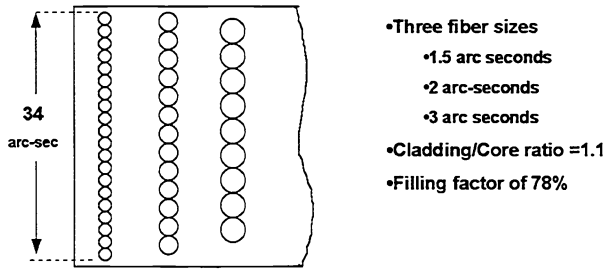

Figure 4: Illustrated here is the fiber layout for the synthetic slit fiber probe.

3.1.3 MOS Light Feed

A 10 probe MOS system will be implemented after the single object and synthetic slit probes. In our baseline design, each probe will have two 1.5", 2", and 3" fibers: one for object and one for sky. Each probe will be carried on an X-Y stage, but each stage will only have access to about 20% of the FoV. This creates a more compact system, and still permits acquisition of up to 10 objects, either concentrated near the center of the FoV or distributed over it. Telecentric compensation will be needed, but can be uni-directional as each probe is constrained within a fraction of a quadrant. An additional probe can have a coherent bundle, for guiding and bore-sighting.

3.2 Spectrograph Input

The fibers from the focal plane are currently envisioned to form seven selectable slit blocks; one each for the 1.5", 2" and 3" linear arrays (including single fibers at the end), three for MOS fiber sizes, and a special purpose block for the scrambler. These blocks will be assembled in a manner similar to that described by Brodie et al.[5] and polished flat. The blocks will be located at the collimator focus by a precision stage. A common X-Y-Z precision stage mechanism will position a mask that selects the number of fibers as well as the effective slit width, and thus resolution, used in a given observation. Modeling shows that the mask will need to be within ~0.1 mm of the fiber end to be effective; i.e. mask unwanted fibers and not vignette others. While challenging, modern micropositioner technology make this quite feasible, eliminating the need for intermediate slits and the attendant loss and aberration in transfer optics. Figure 5 illustrates how a slit mask covers a fiber. Also included are measurements of the fraction of light that was transmitted in a test case where a 400 micron fiber was uniformly illuminated with a f/5 beam and collected by a f/4.0 collimator.

The 1.5", 2 and 3" fibers correspond to resolutions of 6800, 5500 and 3650 respectively. We will use masks to implement additional resolution options of 10900, 15000 and 18000. The fiber slicer will yield a resolution of 21000. The best fiber/mask to use depends on the observation. Consider the following scenario: we want to observe an object much fainter than sky at R~3600. To reduce sky contamination and maximize SNR, a smaller fiber/mask may be optimal even if it produces higher than desired resolution. In this case, on-chip binning can be employed to recover the preferred resolution.

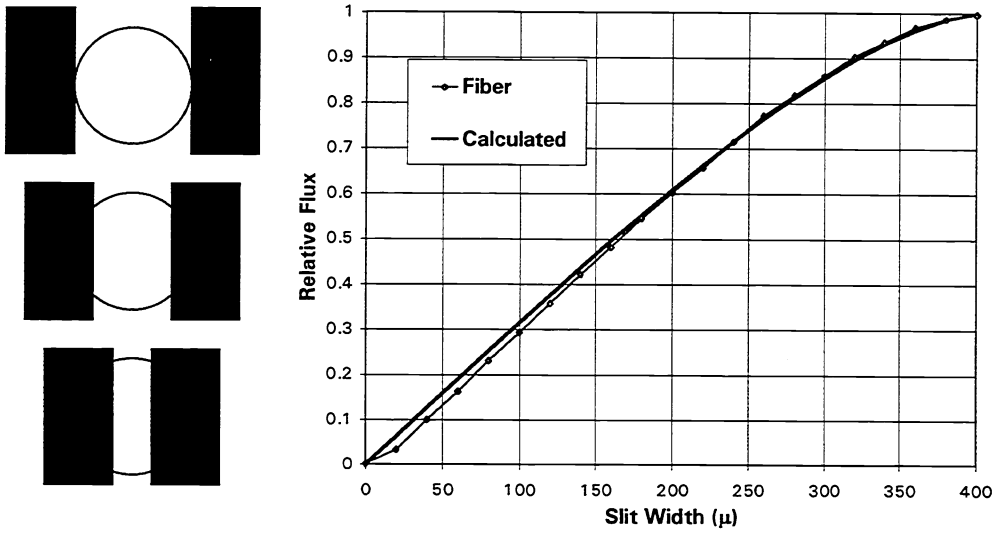

Figure 5: The sketch on the right hand side shows how the slit masks the output of a fiber. The above plot shows laboratory measurements for a uniformly illuminated 400 micron fiber acculted with a slit mask.

3.4 MRS Spectrograph Approach

3.4.1 First Order Design Options

Initial constraints on the MRS design are obtained by investigating the throughput-resolution product for a slit limited spectrograph given by Schroeder[11], whose notation we adopt throughout this proposal:

$$R\phi = 2\,(\sin\theta_B \cos\theta/\cos\alpha)(d/D) \qquad (1)$$

where ϕ is the angle projected on the sky by the entrance aperture, θ_B is the grating blaze angle, α is the incident angle, θ is the difference between the incident and blaze angle (α-θ_B), D is the telescope diameter, and d is the spectrograph collimator diameter. We note, however, that the above equation does not strictly apply to the HET. In equation (1) the spectrograph focal ratio f is matched to that of the telescope; that is $f_{telescope} = f_{collimator}$. This is not true in a fiber coupled spectrograph, as focal ratio degradation in fibers[3] causes $f_{output} < f_{input}$. In addition, both the HET aperture and anamorphic beam shape vary over the course of an integration[1] so that D in equation (1) is not well defined. To correct for these effects, we note that fibers are very good azimuthal scramblers[9] and that the output f of the fiber will always reflect largest angle inserted into it. Thus we can assign D to be the maximum aperture of the HET (D_{max}=9 m) and treat the output beam as circularly symmetric. If we then define $\xi = f_{output}/f_{input}$ equation (1) becomes

$$R\phi = 2\xi(\sin\theta_B\cos\theta/\cos\alpha)(d/D_{max}) \quad (2)$$

There is an extensive literature on design considerations for echelle spectrographs[11,12,13]. The $R\phi \sim 10000$ arc-second target for the MRS is attained readily with ~100 mm beam and standard 63.5° blaze echelles. *We choose echelles as they are the only way to simultaneously meet our spectral coverage and resolution requirements.* Design studies by the author have further narrowed our options to a grating cross dispersed system. This is driven by the need for large order separation, which comes from the requirement for excellent sky subtraction and multiple object work. Prisms are well matched to echelles and do have high efficiency, but a number would be required (2-6) to meet our design goals. We have rejected this approach for the present, but will re-visit it during the design optimization phase.

Further design limitations come from practical considerations. Our spectrograph must use existing rulings. This requirement is driven by the need to have part of the MRS functioning when HET commences science operations in 1997. Consequently, the beam size of the MRS is limited by the availability of cross dispersers and our strong desire not to mosaic them. (Since we must have several cross dispersers, mosaicing will be costly.) Lastly, the fiber fed nature of the spectrograph requires an un-obstructed camera, undoubtedly refractive. *Thus the MRS baseline is a grating cross dispersed echelle with a refractive camera feeding a single large CCD.*

We employ a dual beam spectrograph where a dichroic beamsplitter in the collimator beam divides the MRS into red and blue beams at about 590 nm. There are three compelling arguments to adopt a dual beam design. First, the required wavelength range of 350-1100 nm is a factor of 3.14; far beyond the factor of 2 over which orders are separable with gratings and the blaze function of a single order is efficient. The second argument centers on the cameras. It will be much easier to optimize fast refractive cameras and anti-reflective coatings for image quality and efficiency with the diminished band-pass requirements of a dual beam system. This will result in lower fabrication cost. The third argument grows out of the HET design. The same considerations that lead to a telescope cost reduction of ~75% limits the time an object will be accessible in a given 24 hour period. It is vital to maximize the information rate during that time and, indeed, some science programs require simultaneous full spectral coverage. *A dual beam system is the most cost effective way to meet the science objectives.*

3.4.2 Spectrograph Geometry

Ramsey[14] has carried out an extensive study of over 40 different spectrograph layouts with efficiency as the dominant consideration. Included in his modeling were the blaze efficiency of the echelle[12,15], the blaze efficiency of the cross-disperser at the angles employed, and the vignetting imposed by the finite size of existing rulings. Based on these models, we were forced to abandon the standard in-plane or quasi-Littrow approaches that have typified nearly all echelle systems. These configurations all had substantial losses due to vignetting on the cross-disperser off the echelle blaze peak, and produced low average efficiencies across an order. Even if we relaxed our stance against a mosaic cross disperser the camera speeds required (<f/1) would still be challenging! Instead we turned to the white pupil approach[16]. Widely used in Europe, Tull et al.[17] have demonstrated the strengths of this approach in the McDonald 2-d Coude system. Critics of this design react to the extra reflections in the transfer optics, but our analysis shows, even with these extra reflections, a white pupil design is 25% more efficient than the best in-plane or quasi-Littrow arrangement. *We have no doubt that a white pupil design represents the most efficient and cost effective path to meet our requirements.*

3.4.3 Spectrograph optical design detail

In our baseline design we modified the layout utilized by the ESO high resolution spectrograph for the VLT[18,19], exploiting the symmetries of that approach. Figure 6 shows the optical layout for the red spectrograph, which illustrates the design while presenting the most difficult problem because of the higher angular widths of the orders. The collimator is at the lower right and is illuminated by an array of fibers that is perpendicular to the plane of the paper. The echelle grating is used with a small in-plane angle of θ=5°, with the center of each order along the axis of the first parabolic transfer mirror. This mirror has a

focal length of 2 m and its axis is half way between the echelle and cross disperser. This yields a perfect image at the intermediate focus. Transfer mirror 2, identical to 1, re-collimates the beam. The transfer mirrors together re-image the "white" pupil that the collimator places on the echelle onto the cross disperser grating. The cross disperser need be no larger than the pupil diameter on the echelle times the anamorphic magnification due to the echelle. The camera, in turn, has a well defined entrance pupil at the cross disperser. We note that the transfer mirrors are shown as full mirrors in Figure 6, 7 and 8 but will be fabricated as off-axis parabolas.

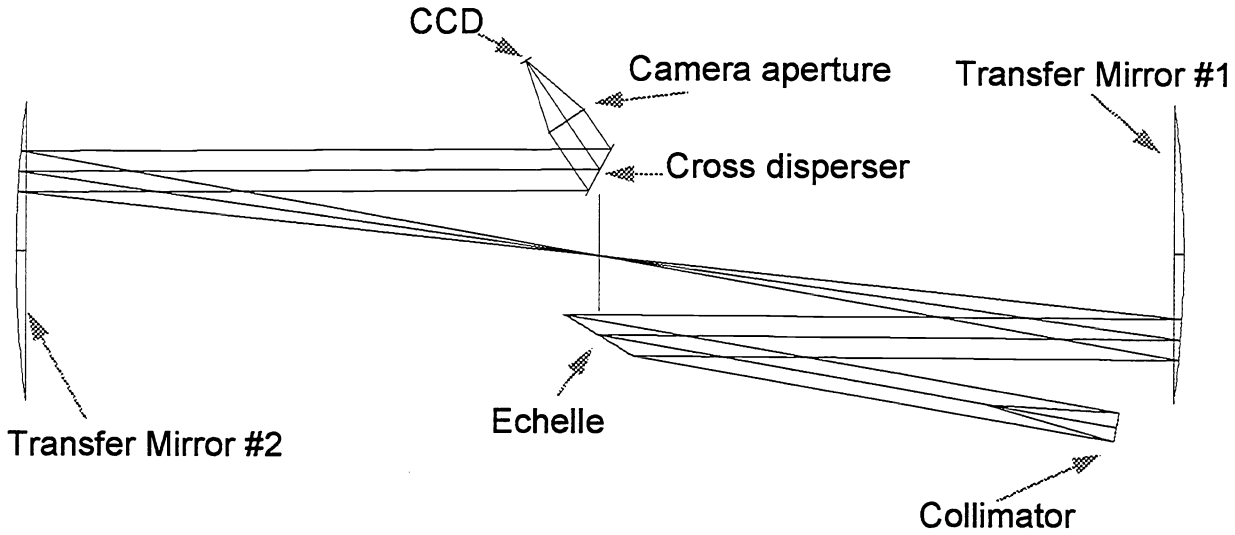

Figure 6: MRS basic layout. This illustrates the path of the mid-order wavelength which is parallel to the axes of the transfer mirrors. The echelle and cross disperser are symmetric about the focus of transfer mirrors 1 and 2. In this case, the intermediate focus is aberration free.

In most echelle systems, the cross disperser and camera are in a diverging beam which increases their required sizes or introduces vignettting. This is often controlled by using coarsely ruled echelles where the angular width of an order is small. Because the MRS's MOS and sky subtraction requirements demand increased order separation, our design must use a more finely ruled echelle with a larger free spectral range (FSR). This is a critical driver in our design. We thus adopt a 79 l/mm echelle which allows good order separation, yet makes effective use of CCD real estate. A 98.7 l/mm echelle would be better for the blue beam, but the current catalog product is too small. We intend to follow this up with Milton Roy as they are re-ruling some echelles..

Figure 7 shows a side view of the MRS for order 23, our worst case order. The figure has three beams traced through it; the central wavelength of the order and wavelengths at +/ - 1/2 FSR. The centers of the echelle and cross dispersers are separated by 580 mm giving comfortable clearances. Due to the large angular width of order 23, the anamorphic magnification varies from almost unity at the high wavelength end to nearly 1.5 at the low wavelength end. The latter number sets the maximum beam size for no vignetting on the cross disperser. The high and low wavelengths are off-axis but the aberrations introduced are small for two reasons. First, the monochromatic beam f ratios are large (f/12.4 or greater). Secondly, the echelle acts as a stop at the focus of transfer mirror 1, that shifts only slightly as a function of wavelength within an order. Transfer mirror 2, being the same focal length as 1, removes coma exactly, leaving field curvature and a small amount of astigmatism. These are correctable in the camera. The cross-disperser is located one focal length from transfer mirror 2.

Since we have chosen to have all the fiber axes parallel and not telecentric, the width of the echelle and transfer mirrors is set by the length of the fiber array at the collimator focus. *In this arrangement, a stop at the collimator focus eliminates field aberrations; this is essential for good sky subtraction.* The fiber array length, or slit length, is set at 20 mm.

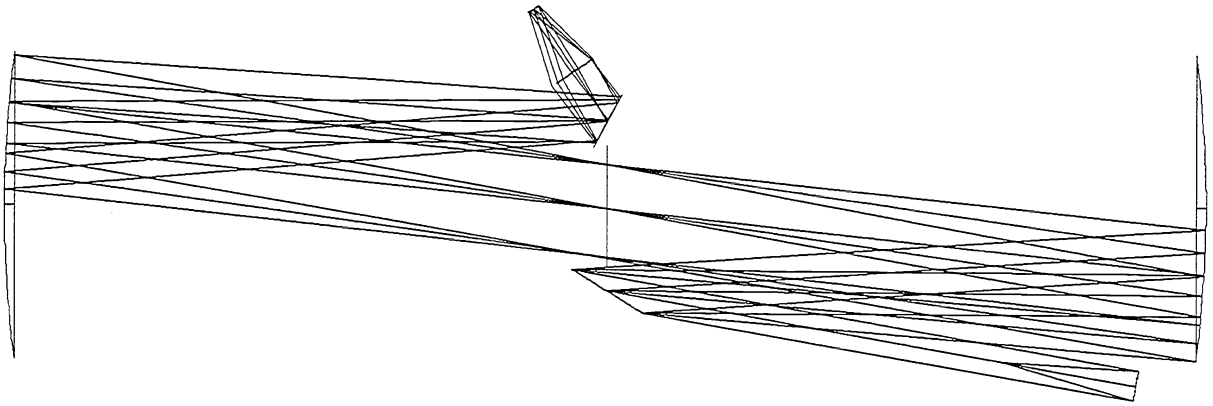

Figure 7: In this figure we illustrate the path of the mid-order wavelength and for high and low wavelengths of order 23 in the red beam.

3.4.4 Camera and Collimator

The optical imaging performance of the spectrograph is dominated by the camera and the collimator. As noted above, the collimator is theoretically aberration free and the transfer mirrors introduce negligible aberration even in the worst case. We have illustrated the collimators as on-axis paraboloids in the above figures but they will be implemented as off-axis paraboloids. The camera used in the above illustrations is a dummy. A major part of the remaining design effort will be to optimize the red and blue camera designs. The baseline camera has a focal length of 250 mm and an f ratio of f/1.4. Several highly efficient all refracting designs of similar size exist in the literature[19,20,21] and will provide very useful starting points.

3.4.5 Dual beam implementation:

The red and blue beams are mechanically orthogonal with the dichroic beamsplitter located in the collimated beam above the collimator focus at the field stop. Wavelengths greater than ~590 nm will be transmitted while those shortward of ~590 nm will be reflected at 90° into the blue spectrograph. The dichroic will also serve as an order sorting filter for the high dispersion cross disperser in the blue beam. Differences in the blue and red beam properties are given in Table 1.

3.4.6 Cross dispersers:

One must recognize that the goals of full spectral coverage and large order separation for sky subtraction or MOS are orthogonal. While both goals can be achieved with costly CCD arrays and wide field cameras, our design meets these goals by using two cross dispersers, one optimized for maximum spectral coverage and the other for maximum order separation. The MRS will also allow us to place narrow band interference filters after the fiber output and obtain up to 90 spectra from 1" fibers arranged in a 2-D array at the telescope focus. In order to meet our high stability requirements, each cross disperser must be automatically installable on a kinematic mount.

3.4.7 Baffles and Exposure Meter:

The intermediate focus between the transfer mirrors is an excellent place for a stray light mask. The mask will have a height (distance perpendicular to dispersion) and width (distance along the dispersion) set by the lowest order in each beam. For the red system, this is about 80 mm by 300 mm. The blue mask will have the same 80 mm height, but will be narrower due to the lower angular spread of the bluer orders.

An exposure meter will be required to guarantee high operational efficiency with the MRS. Preliminary estimates indicate it may be possible to locate coherent fiber bundles at the ends of each mask in the dispersion direction. Since the width of each mask is one FSR for the lowest order and >1 FSR for all other orders, the light level here will be much lower (~1%) than in the order peak, but a modest size fiber bundle and lack of cross dispersion will allow a significant bandwidth to be sampled. Although this signal will be biased toward the reddest orders in each beam, it should be adequate for metering.

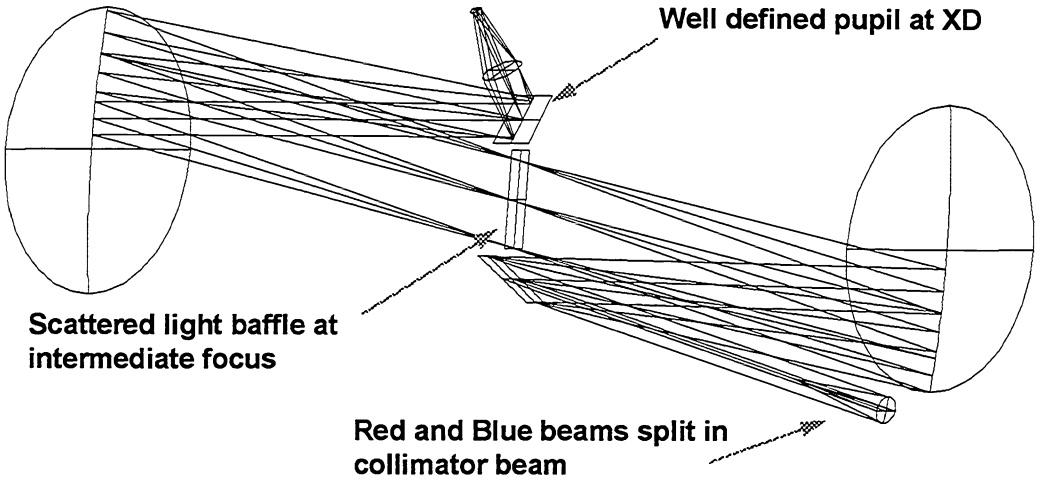

Figure 8: Perspective MRS basic layout which illustrates some of the features of the design. Particularly apparent in this view is the intermediate focus.

3.4.7 Design Summary

Table 1 summarizes the baseline design for the MRS.

Table 1

Summary of MRS properties

Resolution = 10666 arc-seconds	$\theta = 5°$	$\gamma = 0°$
Collimator		
Diameter	120 mm	
Focal length	450 mm	
	Red Beam	**Blue Beam**
Camera		
Focal length	250 mm	250 mm
F ratio	f/1.4	f/1.5
Transfer Parabola		
Focal length	2000 mm	2000 mm
Clear aperture	500 mm	500 mm
Echelle		
Size	125 x 260 mm	125 x 260 mm
lines/mm	79	79
Blaze angle	63.43°	63.43°
Cross Disperser		
Grating	400 l/mm, Θ_b =9.7°	400 l/mm, 2nd order, Θ_b =9.7°
Wavelength Coverage	578 to 1098 nm	350 to 648 nm

3.5 CCD geometry

The MRS will achieve its best performance utilizing the emerging 4096x2048 15μm pixel CCDs. With the baseline camera, the CCDs will critically sample at a resolution of 28000. A one arc-second fiber will project to 5.32 pixels. The echelle format will require two such CCDs in the red camera but only one in the blue beam. Figure 9 illustrates the echelle format for both the blue and red beams.

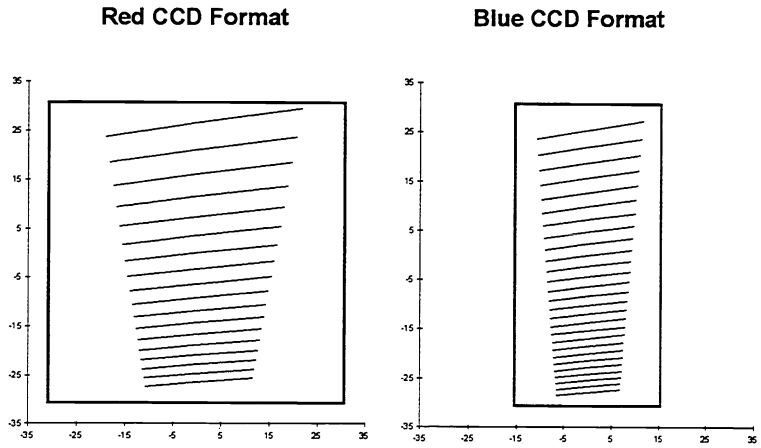

Figure 9. Spectral order maps for the red beam of the MRS (left side) and the blue beam. Note that the red detector size is outlined and will consist of two 4096 x 2048 CCDs. A single CCD will suffice for the blue beam.

3.6 Performance

Figure 10 summarizes the efficiencies for the HET system as well as the spectrograph. The efficiency of the MRS on the HET, including everything but fiber input losses due to seeing, will peak at about 20%. It is higher than 10% from 440 to 850 nm. This very high performance for an echelle system is made possible by silver coatings on most of the blue side components and on all of the components of the red system. In addition we intend to silver overcoat the gratings, at least in the red spectrograph. While there is some risk in this, the grating component costs are not so high as to preclude re-replication. As a validation of our modeling procedure, we used it to predict the measured 8% efficiency of the Keck with HIRES[22]. Our model agreed with the measured HIRES efficiency within 15%.

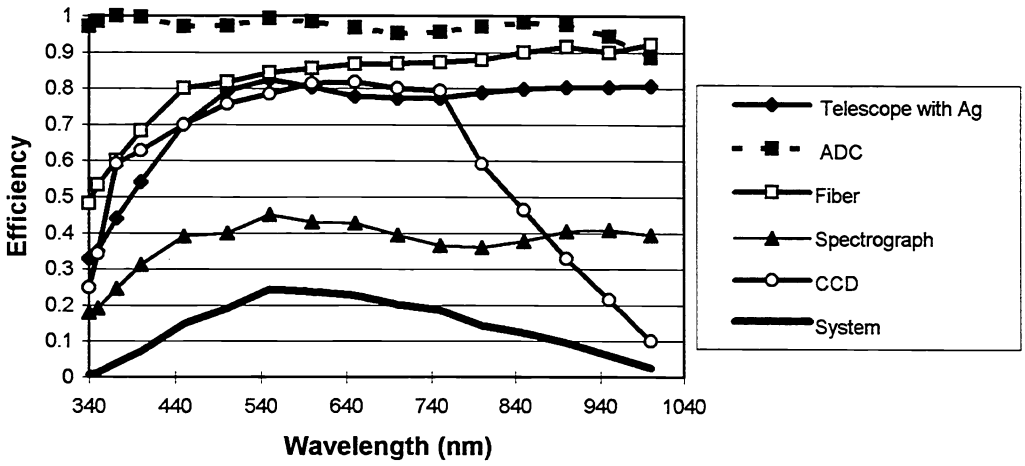

Figure 10: Modeled efficiency of the HET & MRS at order peaks exclusive of seeing losses at the fiber input. The peak efficiency is at ~20%. Also given are the components that contribute to the efficiency: the telescope, the transfer optics, fiber and CCD. The high overall value is due in part to the extensive use of silver coatings.

The SNR per pixel in a 3000 second integration for a point source as a function of V magnitude for the HET and MRS is given in Figure 5. For these calculations, we use a MRS efficiency of 15% for resolutions 3000, 6000 and 12000. There are three pixels per resolution element. We use a 1" seeing profile[8] to calculate the amount of light inserted into the fiber. A continuum sky brightness of V=21.97/arc-sec^2 is assumed.

A vital performance area for the MRS will be in sky subtraction. Barden et al.[4] and Wyse & Gilmore[23] discuss the issues involved with fiber sky subtraction. The MRS design will be superior in this regard for the following reasons. First, we pay attention to the illumination of the fibers at the telescope focus to assure proper telecentric illumination. Secondly, we control the field aberrations in the collimator and the white pupil design properly places pupils on the gratings and eliminate field dependent vignetting. Lastly, the optical bench approach eliminates variable flexure. These are the major factors that have led to the perception that one cannot do quality sky subtraction with fibers. *We are confident that careful attention to the details described above will lead to a system with sky subtraction capability equal or exceeding that obtained with conventional slit spectrographs.*

3.7 Upgrade Potential

The dual beam white pupil approach taken here gives the MRS a good deal of modularity, thus facilitating upgrades. We can already envision upgrades that have not been made part of this project: two are listed below:

- *Implementation of a 2-D Fiber Array*: We can accommodate nearly one hundred 1" fibers in our collimator field: this upgrade can be performed with the addition of another slit block and an accompanying cable to the HET focal plane. This opens up some extremely interesting areas of galaxy dynamics, particularly at intermediate redshifts.
- *NIR Spectroscopy*: With a well defined pupil at the cross disperser, an IR capable camera an NIR array can extend the useful range of the MRS through the H band. This region is largely un-exploited especially at the high end of the MRS resolution capability.

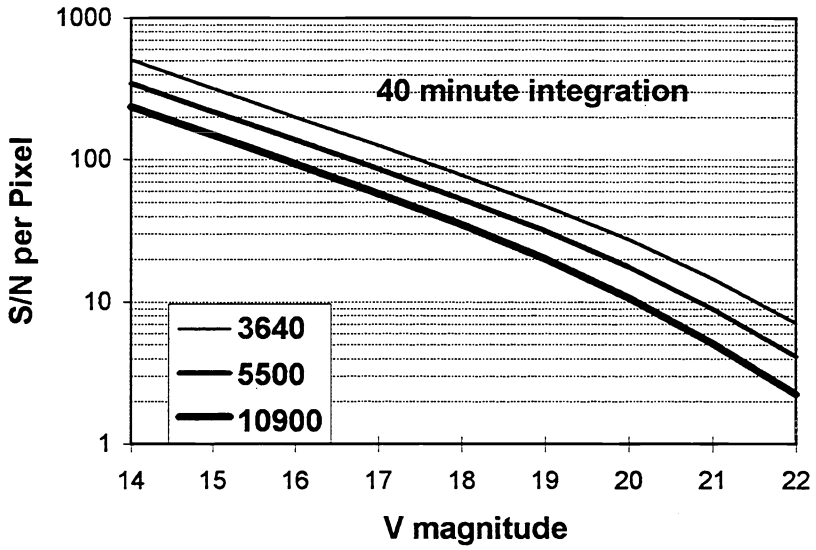

Figure 11. This figure is modeled performance of the MRS at R= 3640, 550 & 10900 in 1 arc-second seeing at the 15% efficiency that is typical across most of the visible band. The S/N per pixel with 3 pixels per resolution element. Sky is V= 21.9/arc-sec^2.

4. REFERENCES

1. Ramsey, L.W., Sebring, T.A., & Sneden, C., 1994, "The Spectroscopic SurveyTelescope Project", S.P.I.E. Vol. 2199, *Advanced Technology OpticalTelescopes V*, p. 31..

2. Sebring , T.A., Booth, J.A., Good, J.M., Krabbendam, V.L. and Ray, F.B. "Design and Status of the Spectroscopic Survey Telescope", *Advanced Technology Optical Telescopes* V, SPIE Tech. Conf. 2199, Kona, HI, 1994..

3. Ramsey, L.W. 1988, "Focal Ratio Degradation in Optical Fibers of Astronomical Interest", in ASP Conf. Ser.~3, *Fiber Optics in Astronomy*, ed. S. Barden, (San Francisco: Astronomical Society of the Pacific), p. 26.

4. Barden, S.C. Armandroff, T., Massey, P., Groves, L., Rudeen, A.C., Vaughnn, D.,& Muller, G. 1993, ``Hydra -- Kitt Peak Multi-Object Spectroscopic System",in *ASP Conf. Ser. 37, Fiber Optics in Astronomy II*, ed. P.M. Gray, (San Francisco: Astronomical Society of the Pacific), p. 185.

5. Brodie, J.P. Donnelly, R.H., Epps, H.W. Radovan, M.V. & Craig, W.W. 1994,``Efficiently Mating Fibers to Spectrographs," *S.P.I.E.* Vol 2198, Instrumentation in Astronomy VII, p. 21.

6. Brodie, J.P., Lampton, M. & Bowyer, S. 1988, ``Optimum Choice of Fiber Diameter for Multiple-Object Spectroscopy", *AJ* 96, p. 2005.

7. Ingerson, T.E. 1993, "Asssessing the Performance of ARGUS-CTIO's Multiple Object Spectrometer", in ASP Conf. Ser. 37, *Fiber Optics in Astronomy II*, ed.~P.M. Gray, (San Francisco: Astronomical Society of the Pacific), p. 76.

8. Diego, F. 1985, ``Stellar Image Profiles from Linear Detectors and the Throughput of Astronomical Instruments", Pub. Astro. Soc. Pacific 97, p. 1209.

9. Hunter, T.R., & Ramsey, L.W. 1992, "Scrambling Properties of Optical Fibers and the Performance of a Double Scambler", PUB ASTR. SOC. PACIFIC 104, p. 1244.

10. Wynne, C.G. 1993, ``Telecentricity in Fiber-Fed Spectrographs," Mon. Not. Royal Astr. Soc. 260, p. 307.

11. Schroeder, D. 1987, *Astronomical Optics*, (San Diego: Academic Press).

12. Walker D.D., & Diego, F. 1985, "Design Philosophy of the Forthcoming EchelleSpectrographs for the AAT and LPO", Mon. Not. Royal Astr. Soc. 217, p. 355.

13. Walker, D.D., Radley, A.S., Diego, F., Charalambous, A., Dryburgh, M., &Bigelow, B.C. 1994, ``Reexamination of High-Resolution Spectrographs for Large Telescopes: The Cassegrain Solution", S.P.I.E. Vol. 2198, *Instrumentationin Astronomy VII*, p 1083.

14. Ramsey, L.W. 1994, "HET Medium Resolution Spectrograph Concept Design Study:Optimizing the Optical Layout", HET internal report, HET TR940502.

15. Schroeder, D.J., \& Hilliard, R.L. 1980, ``Echelle Efficiencies: Theory and Experiment", *Applied Optics*, 19,p. 2833.

16. Baranne, A. 1988, "White Pupil Story, or Evolution of a Spectrograph Mounting", in *Very Larg Telescopes And Their Instrumentation*, ed.~M.-H. Ulrich, (Garching: European Southern Observatory), p. 1195.

17. Tull, R.G., MacQueen, P., Sneden, C., & Lambert, D.L. 1994, "The McDonald 2.7-m Echelle Spectrometer", in ASP Conf. Ser. 55, *Optical Astronomy from the Earth and Moon*, ed. D.M. Pyper & R.J. Angione, (San Francisco: Astronomical Society of the Pacific), p. 148.

18. Dekker, H., & D'Odorico, S. 1992, "UVES, the UV-Visual Echelle Spectrograph for the VLT", *ESO Messenger 70*, p. 13.

19. Delabre B. 1993, "ESO-Very large Telescope: UVES Preliminary Optical Design Report", *ESO Doc.~No.~VLT-TRE-ESO-13200-0272*.

20. Epps, H.W. 1988, "Fast Broad-Passband Lenses for Spectrometers on LargeTelescopes", in *Very Larg Telescopes And Their Instrumentation*, ed. M.-H. Ulrich, (Garching: European Southern Observatory), p. 1157.

21. Rodgers, J.M., & McCarthy, J.K. 1994, "Design of a High-Speed UV-Transmitting Camera for the Keck LRIS" S.P.I.E. Vol. 2198,*Instrumentation in Astronomy VII*, p. 1096.

22. Vogt, S.S., Allen, S.L., Bigelow, B.C., Bresee, L., Brown, B., Cantrall, T.,Conrad, A., Couture, M., Delaney, C., Epps, H.W., Hilyard, D., Hilyard, D.F.,Horn, E., Jern, N., Kanto, D., Keane, M.J., Kilbrick, R.I., Lewis, J.W.,Osborne, C.M., Osborne, J., Pardeilhan, G.H., Pfister, T., Ricketts, T.,Robinson, L.B., Stover, R.J., Tucker, D., Ward, J., & Wei, M. 1994, "HIRES: The High-Resolution Echelle Spectrometer on the Keck 10 m Telescope", S.P.I.E. Vol. 2198, *Instrumentation in Astronomy VII*, p. 362.

23. Wyse, R.F.G., & Gilmore, G. 1992, ``Sky Subtraction with Fibers", Mon. Not. Royal Astr. Soc. 257, p. 1.